Front. Earth Sci. 2020, 14(2): 413–429
https://doi.org/10.1007/s11707-019-0780-x

RESEARCH ARTICLE

Modeling grass yields in Qinghai Province, China, based on MODIS *NDVI* data—an empirical comparison

Jianhong LIU (✉)[1,2,3], Clement ATZBERGER[3], Xin HUANG[1,2], Kejian SHEN[4,5], Yongmei LIU[1,2], Lei WANG[1,2]

1 Shaanxi Key Laboratory of Earth Surface System and Environmental Carrying Capacity, Northwest University, Xi'an 710127, China
2 College of Urban and Environmental Science, Northwest University, Xi'an 710127, China
3 Institute of Surveying, Remote Sensing and Land Information, University of Natural Resources and Life Sciences (BOKU), Peter Jordan Straße 82, Vienna 1190, Austria
4 Remote Sensing Center for Agriculture and Animal Husbandry of Qinghai, Xining 810007, China
5 Chinese Academy of Agricultural Engineering Planning and Design, Beijing 100125, China

Abstract Qinghai Province is one of the four largest pastoral regions in China. Timely monitoring of grass growth and accurate estimation of grass yields are essential for its ecological protection and sustainable development. To estimate grass yields in Qinghai, we used the normalized difference vegetation index (*NDVI*) time-series data derived from the Moderate-resolution Imaging Spectroradiometer (MODIS) and a pre-existing grassland type map. We developed five estimation approaches to quantify the overall accuracy by combining four data pre-processing techniques (original, Savitzky-Golay (SG), Asymmetry Gaussian (AG) and Double Logistic (DL)), three metrics derived from *NDVI* time series (VI_{max}, VI_{season} and VI_{mean}) and four fitting functions (linear, second-degree polynomial, power function, and exponential function). The five approaches were investigated in terms of overall accuracy based on 556 ground survey samples in 2016. After assessment and evaluation, we applied the best estimation model in each approach to map the fresh grass yields over the entire Qinghai Province in 2016. Results indicated that: 1) For sample estimation, the cross-validated overall accuracies increased with the increasing flexibility in the chosen fitting variables, and the best estimation accuracy was obtained by the so called "fully flexible model" with R^2 of 0.57 and *RMSE* of 1140 kg/ha. 2) Exponential models generally outperformed linear and power models. 3) Although overall similar, strong local discrepancies were identified between the grass yield maps derived from the five approaches. In particular, the two most flexible modeling approaches were too sensitive to errors in the pre-existing grassland type map. This led to locally strong overestimations in the modeled grass yields.

Keywords Qinghai Province, grass yield, remote sensing, MODIS, vegetation index

Received March 25, 2019; accepted July 14, 2019

E-mail: jhliu@nwu.edu.cn

1 Introduction

For the ecological conservation and management of pastoral areas, three indicators are essential: (i) vegetation growth, (ii) grass yields, and (iii) livestock carrying capacity. Grass yield is the basis for determining grassland livestock carrying capacity (Xu et al., 2008; Yu et al., 2010), a precondition for a balanced management of grasslands.

In recent years, climate change and improper grazing have led to grassland degradation at different degrees in Qinghai (Chen et al., 2013; Yin et al., 2014). As indicated by Yin et al. (2014) there were over 120000 km^2 of grasslands in Qinghai which exhibited severe degradation in 2008, and the grass yield per unit area decreased by 30%–50%, compared to their status in the 1950s. At the same time, the proportion of high-quality forage grass decreased by 20%–30%, while the proportion of grasslands with poisonous or harmful weeds increased by 70%–80%. This underlines the importance of a regular (e.g., annual) monitoring of grass yields in Qinghai Province (Li et al., 2015). Similar requirements are also known from other grassland regions of the world.

The traditional method for measuring grass yields is labor-intensive and time-consuming, and therefore impractical for large-scale application. Since the 1990s, researchers have estimated regional changes in grass yields or biomass using statistical models based on remotely sensed vegetation index data, calibrated against ground observed

data (Li et al., 1998; Piao et al., 2007; Rusch et al., 2014; Atzberger et al., 2015; Wehlage et al., 2016). Similar approaches are also employed when evaluating drought effects on grazing conditions (Klisch and Atzberger, 2016) and more generally for agricultural yield and production forecasts (Rojas, 2007; Ren et al., 2008). The studies rely on the relatively strong correlations between grassland yields or biomass and spectral vegetation indices (*VI*s). Remotely sensed vegetation indices are particularly suitable for low biomass environments, as the signal is not yet saturated (Baret et al., 1989).

Among the various vegetation indices, the most commonly used is the normalized difference vegetation index (*NDVI*), which has been proven to be a good indicator for monitoring vegetation growth and activities (Zhou et al., 2001; Piao et al., 2006; Mohammat et al., 2013; Rembold et al., 2013). The index is available across many different sensors and routinely provided in data archives (e.g., GIMMS 3g, going back until 1981 (Pinzon and Tucker, 2010)). Several other vegetation indices were also used to estimate grassland biomass, including ratio vegetation index (*RVI*) (Jordan, 1969), renormalized difference vegetation index (*RDVI*) (Roujean and Breon, 1995), enhanced vegetation index (*EVI*) (Huete et al., 2002), difference vegetation index (*DVI*) (Pearson and Miller, 1972), perpendicular vegetation index (*PVI*) (Tukey, 1977), modified soil adjusted vegetation index (*MSAVI*) (Qi et al., 1994), and optimized soil adjusted vegetation index (*OSAVI*) (Rondeaux et al., 1996). Based on theoretical considerations, potentials and limits of several vegetation indices are summarized in Baret and Guyot (1991) and Xue and Su (2017). For example, *RVI* has a good correlation with vegetation biomass, but is sensitive to atmospheric effects. *NDV*I is the most widely used vegetation index, but is sensitive to soil optical properties.

As different grassland types have their own characteristics, such as grass compositions, soil types, topography, etc., the optimum indices to estimate grass yields may vary from study to study. For example, Li et al. (1998) compared the relationships between *RVI* as well as *NDVI* and the grass yields in Fukang County, Xinjiang Province, China. They found that fresh herbage yields correlated better with *RVI* than *NDVI* for lowland meadow, hill desert steppe, and mountain meadow, but not for plains desert steppe. Duan et al. (2012) investigated the correlations between six vegetation indices and the above-ground biomass of alpine grassland in northern Tibet. Their results showed that *OSAVI* had the best correlation with grassland biomass, while *RVI* had the worst. Yu et al. (2010) estimated the alpine grassland yields in Golog Prefecture, Qinghai Province, using *NDVI* and *EVI* data derived from the Moderate Resolution Imaging Spectroradiometer (MODIS). The result showed the estimation accuracy based on *NDVI* is higher than that based on *EVI*. Similarly, Fu et al. (2013) found that MODIS *NDVI*-based accuracy is higher than MODIS *EVI*-based for all four main grassland types in estimating grass yields in Sichuan Province, China.

The observed lack of agreement between different studies confirms the well-established fact that statistical yield/biomass estimation models are generally sensor, site, and season-specific (Baret et al., 1989; Ali et al., 2016). The lack of generalization is a direct result of the fact that natural conditions (such as temperature, precipitation, soil type, elevation) vary greatly, and therefore "optimum" models vary over space and time. To cope with those shortcomings, physically-based radiative transfer models (RTM) have been used as an alternative for assessing grassland biomass (Darvishzadeh et al., 2008; Darvishzadeh et al., 2011). Although RTM are based on physical principles, they have their own limitations (Baret and Buis, 2008), such as model capacity in accurately describing radiative transfer in canopies and building a realistic training data set.

With respect to statistical models, several papers have shown that nonlinear models often achieve higher accuracy than linear models, especially exponential and power function models (Li et al., 1998; Xu et al., 2008; Wehlage et al., 2016). For the Qinghai grassland region, further research is required to determine which statistical models provide the most accurate estimation of grass yields. More research is also warranted to assess if the maximum, or seasonal/annual accumulation of *VI* should be used for grass yield estimation (Yang et al., 2016; Xun et al., 2018). Most published research uses the maximum vegetation index value within a given growing season for grass yield estimation. However, papers such as Schucknecht et al. (2017) found that a seasonal integration correlates better with pasture availability.

For the current research, we attempted to analyze various empirical models using data from Qinghai Province. As a reference approach, we use the most common approach which is used to calibrate the remotely sensed data against all available in situ data while ignoring grassland types. We call this the "generic approach," against which we compare four different alternative approaches. The chosen alternatives generated grassland type specific models and moreover vary in terms of applied pre-processing, metrics and fitting functions. The nested analysis 1) permits investigation into whether the increase in flexibility enhances the estimation accuracy; 2) examines the grass yield maps derived from different approaches; 3) provides a reference basis for improving grassland management and animal husbandry development in Qinghai Province.

2 Materials and methods

2.1 Study area

Qinghai Province (31°9′N–39°19′N, 89°35′E–103°04′E) is

located in western China, in the north-east part of the Qinghai-Tibet Plateau (Fig. 1). Qinghai has two cities and six prefectures under its jurisdiction. It is the source of three major river systems (the Yellow, Yangtze, and Lancang Rivers), and is therefore known as the "Water Tower of China." The region's average elevation is 3000 m above sea level. It has a typical plateau continental climate characterized by short summers, with average annual temperature ranging from −6°C to 9°C and average annual precipitation of 250–550 mm. The grass growing season usually starts from early May and ends at the end of October. According to the second grass resources survey of Qinghai, its natural grassland covers an area of 41.9 million ha, accounting for 10.7% of China's total grassland area, making it the country's 4th largest pastoral region (Qinghai Provincial Grassland Station, 2012). The natural grassland that can be used for grazing or production is 38.6 million ha, which mainly located in the Qinghai-Tibet Plateau, Qilian Mountain, and Qaidam Basin.

An actual grassland type map (Fig. 1) was obtained from the Geomatics Center of Qinghai. It was compiled by Qinghai Provincial Grassland Station and Geomatics Center of Qinghai. The map reflects the vegetation cover and soil properties in Qinghai province up to 2011, based on survey results of the General Grass Survey Station of Qinghai (Qinghai Provincial Grassland Station, 2012). The main grassland types include alpine steppe, alpine meadow, and alpine desert. As the class "alpine meadow" occupies more than half of the vegetated area, this grassland type was split into three sub-strata (alpine meadow-high, alpine meadow-medium, and alpine meadow-low in Fig. 1) using the natural breaks method packaged within GIS software (Jenks and Caspall, 1971; de Smith et al., 2018), according to the elevation.

2.2 Data sources

2.2.1 Ground survey data

The ground survey (*in situ*) data were collected by the Qinghai Grassland Supervision Center between July 20 and August 31, 2016. The dates reaching the maximum biomass are different for grassland in different locations. As the area of Qinghai Province is vast, the peaking time differs from south to north, east to west. Field measurements were carried out when the grassland reached its peak time, according to the monitoring of local grassland

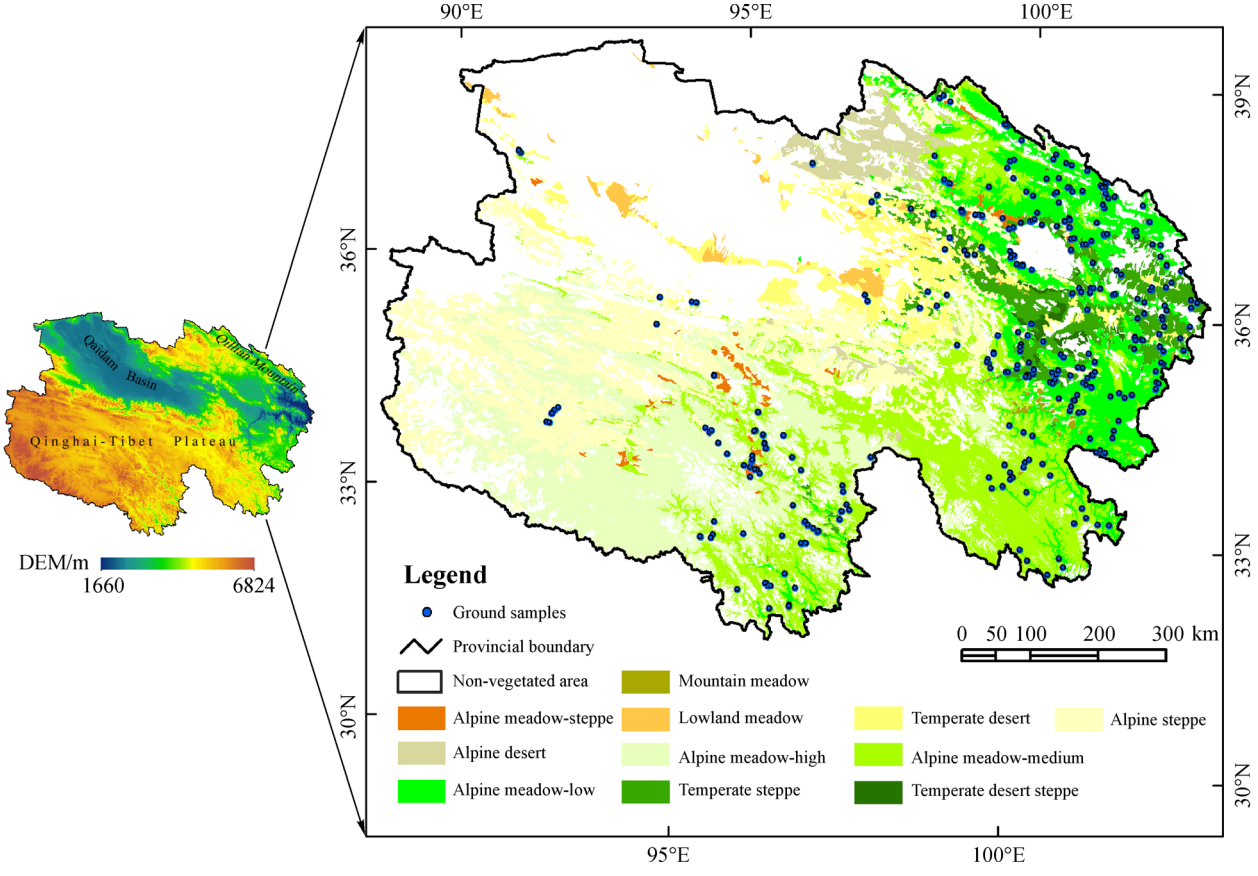

Fig. 1 Location, elevation and grassland types of research area. The blue dots show the ground survey samples in 2016. Note that the main grassland biome of "alpine meadow" was sub-divided for this study into three (height-dependent) strata, as this grassland type is spread over a wide elevation range.

management units. Information of the survey samples included locations, grassland types, fresh grass yields, and altitudes. Samples were randomly located in the unused homogeneous areas of typical grassland, on the condition of accessibility. In remote areas with high elevation and no roads, there were fewer samples. In each 100 m × 100 m sample, three 1 m × 1 m plots were chosen in different locations. The fresh grass yields of three plots were then averaged and recorded as the yield of one sample. To ensure the reliability of the ground samples, we excluded any samples lacking latitude, longitude, or grassland type. In cases where two or more samples fell within one MODIS pixel, the averaged grass yield was used as one sample. After this screening, the total number of samples was 556 (blue dots in Fig. 1). Detailed information about grassland acreage and available samples within each grassland type is shown in Table 1.

No ground sample data was available for the following four grassland types: lowland meadow, mountain meadow, temperate desert steppe, or alpine desert. Since these grassland types only cover small areas in Qinghai province, respectively, and are located in remote areas (Fig. 1), they were excluded from further analysis. Therefore, in total, we distinguished seven grassland types (IDs 1 to 7 in Table 1). Sample density differs among grassland types due to accessibility. The standard deviations of grass yields for samples in high production grassland types generally are higher than that of lower production types.

2.2.2 Remote sensing data

For analysis, MOD09Q1 time series covering 2016 were downloaded from the US Geologic Survey (available at USGS website). The data had a temporal resolution of eight days and a spatial resolution of 250 m. The MODIS Reprojection Tool and *ENVI* software were used for data pre-processing. Red, near-infrared reflectance bands as well as the quality band were extracted to compute the *NDVI* and assist data processing.

2.3 Smoothing of *NDVI* time series and metrics

MODIS *NDVI* time series was processed in four different ways: the original *NDVI* time series with only linear interpolation (denoted as *NDVI*_O), and *NDVI* smoothed with Savitzky-Golay (Chen et al., 2004) (denoted as *NDVI*_SG), asymmetric Gaussian (Jönsson and Eklundh, 2002) (denoted as *NDVI*_AG) and double logistic (Beck et al., 2006) (denoted as *NDVI*_DL). To detect noises in the *NDVI* time series, we used the quality file included within the data set (Vermote et al., 2015). *NDVI* with the reflectance state marked as "clear" was labeled as good quality, "mixed" as medium quality, and "cloudy" or "cloud shadow" as poor quality. *NDVI*_O replaced *NDVI* values of poor quality with linear interpolation. The three smoothing algorithms were investigated, which often used in similar studies (useful comparative studies are provided in Gao et al. (2008), Hird and McDermid (2009), and Atkinson et al. (2012)). In this paper when using TIMESAT 3.3 for *NDVI* smoothing, the quality flags were also used to set the weights. For *NDVI* values with good quality, medium quality, and poor quality, the weights were set to be 1.0, 0.5 and 0.1, respectively. In the filtering process, no spike method was applied. The number of envelope iterations and adaptation strength were both set to be 2, because lower parameters tend to underestimate the *NDVI* time series and higher parameters tend to overestimate *NDVI* time series. These settings were the same for Savitzky-Golay (SG), asymmetric Gaussian (AG), and double logistic (DL) filtering. Additionally, the window size for SG filtering was set to 4, as recommended by Chen et al. (2004).

Temporal *NDVI* profiles from temperate steppe, alpine meadow-steppe, alpine steppe, temperate desert, alpine meadow-low, alpine meadow-medium, and alpine meadow-high are shown exemplarily in Fig. 2(a). Each curve is the average calculated over all survey sample pixels. Overall, the seven grassland types present very similar growth cycles with, however, some noticeable shifts in the timing of onset and peak height. The growing season was from early May to early November in 2016, according to

Table 1 Acreage and field samples of each grassland type

Grassland types	ID	Acreage/km^2	Sample number	(Acreage/Sample)/km^2	Mean yield/(kg·ha^{-1})	Standard deviation/(kg·ha^{-1})
Temperate steppe	1	26603	101	263.4	2377.0	1163.0
Alpine meadow-steppe	2	3940	21	187.6	1445.6	657.6
Alpine steppe	3	96915	50	1938.3	1687.0	1158.5
Temperate desert	4	27469	25	1098.8	1279.7	1277.3
Alpine meadow-low	5	60127	233	258.1	3715.3	1594.6
Alpine meadow-medium	6	104909	108	971.4	2471.9	1457.1
Alpine meadow-high	7	111312	18	6184.0	1607.7	1052.1
Σ		452797	556	814.4	2784.8	1644.63

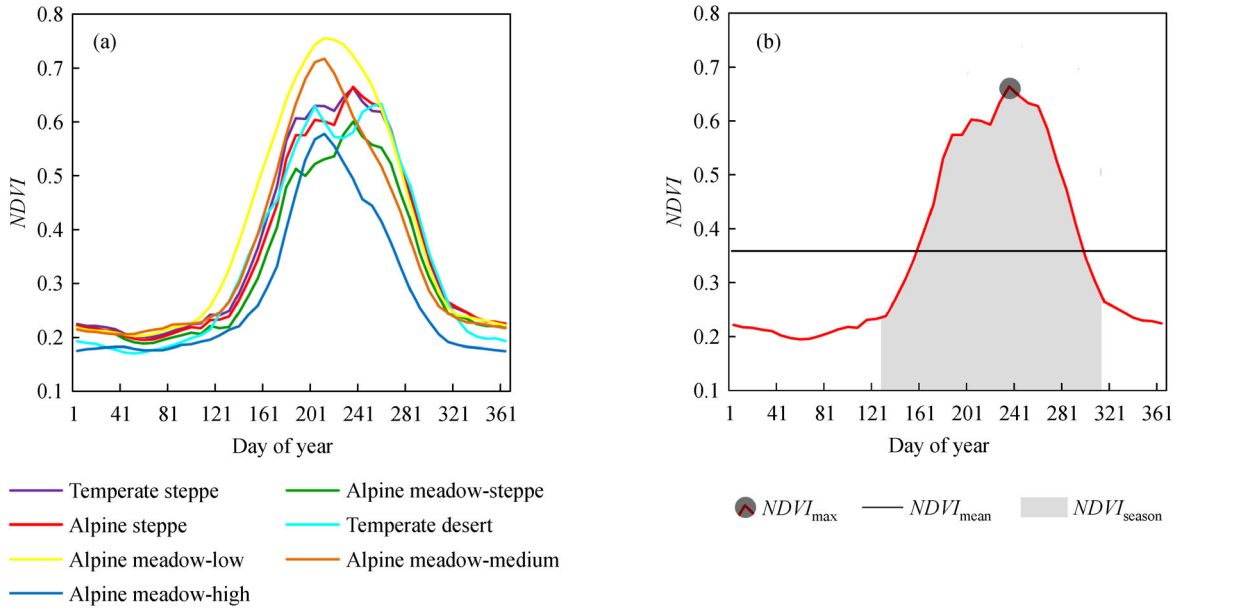

Fig. 2 (a) Temporal profiles of the seven investigated grassland types. The curves are derived from the Savitzky-Golay smoothed NDVI time series with 8-day temporal resolution in 2016. (b) schematic drawing of the three metrics, $NDVI_{max}$, $NDVI_{season}$ and $NDVI_{mean}$.

local grassland monitoring units. It also can be seen in Fig. 2(a). On average, grass began their rapid growth around Day of Year (DOY) 219 (that is May 8), reached the peak of growth around DOY 241 (that is August 28), and senesced around DOY 313 (that is November 8) (Fig. 2(b)). Though the peaking time differs largely from one grassland type to another, the green-up time and senescence time is quite close. Therefore, based on Fig. 2(a), the grass growing season is determined from May 8 to November 8 in 2016.

To model fresh grass yield for each pre-processing, three metrics (as shown in Fig. 2(b)), were calculated and used for subsequent analysis:

1) the maximum *NDVI* value within the growing season, denoted as $NDVI_{max}$;

2) the cumulative *NDVI* value of the growing season, denoted as $NDVI_{season}$;

3) the mean value of *NDVI* for the entire calendar year, denoted as $NDVI_{mean}$.

2.4 Empirical modeling

The general flowchart and the various models assessed in this study are shown in Fig. 3. The figure highlights the four pre-processings, three *NDVI* metrics, four fitting functions and two categories of models leading to five estimation approaches (Table 2): 1) the generic approach, 2) the fixed fitting function approach, 3) the fixed metric approach, 4) the fixed pre-processing approach and 5) the fully flexible approach:

- pre-processings: *NDVI*_O, *NDVI*_AG, *NDVI*_DL and *NDVI*_SG
- metrics: $NDVI_{max}$, $NDVI_{annual}$ and $NDVI_{season}$
- fitting functions: linear, 2nd order polynomial, power and exponential
- models: generic models, grassland type-specific models

In total, we analyzed four pre-processed *NDVI* time series: *NDVI*_O, *NDVI*_AG, *NDVI*_DL, and *NDVI*_SG. Based on these four pre-processings, we calculated three kinds of metrics, i.e. $NDVI_{max}$, $NDVI_{mean}$ and $NDVI_{season}$ (Fig. 2). Thus, the maximum *NDVI* value derived from the SG-smoothed data was for example denoted as $NDVI\_SG_{max}$. Four fitting functions were explored: the linear model, the 2nd order polynomial model, the power model, and the exponential model.

Two categories of models were calibrated (Table 2): generic models and grassland type-specific models. We first calibrated models that did not differentiate grassland types, called “generic” models. Grass yield estimation was afterwards done for each grassland type separately, as type-specific grass yield models generally outperform those that pool all the data together (Xu et al., 2008; Duan et al., 2012). For all models, the calibration was conducted based on the input pre-processing, metric, and fitting function using cross-validation by the coefficient of determination (R^2) and the relative root mean square error ($RMSE_R$) for assessing the model performance (Lobell and Asner, 2004). After that, we investigated overall grass yield estimation accuracy (R^2 and the root mean square error (*RMSE*)) of all available ground samples through five different approaches (Table 2). Then we produced the best yield estimation maps using the five approaches. Finally, we obtain an averaged grass yield map from the five best

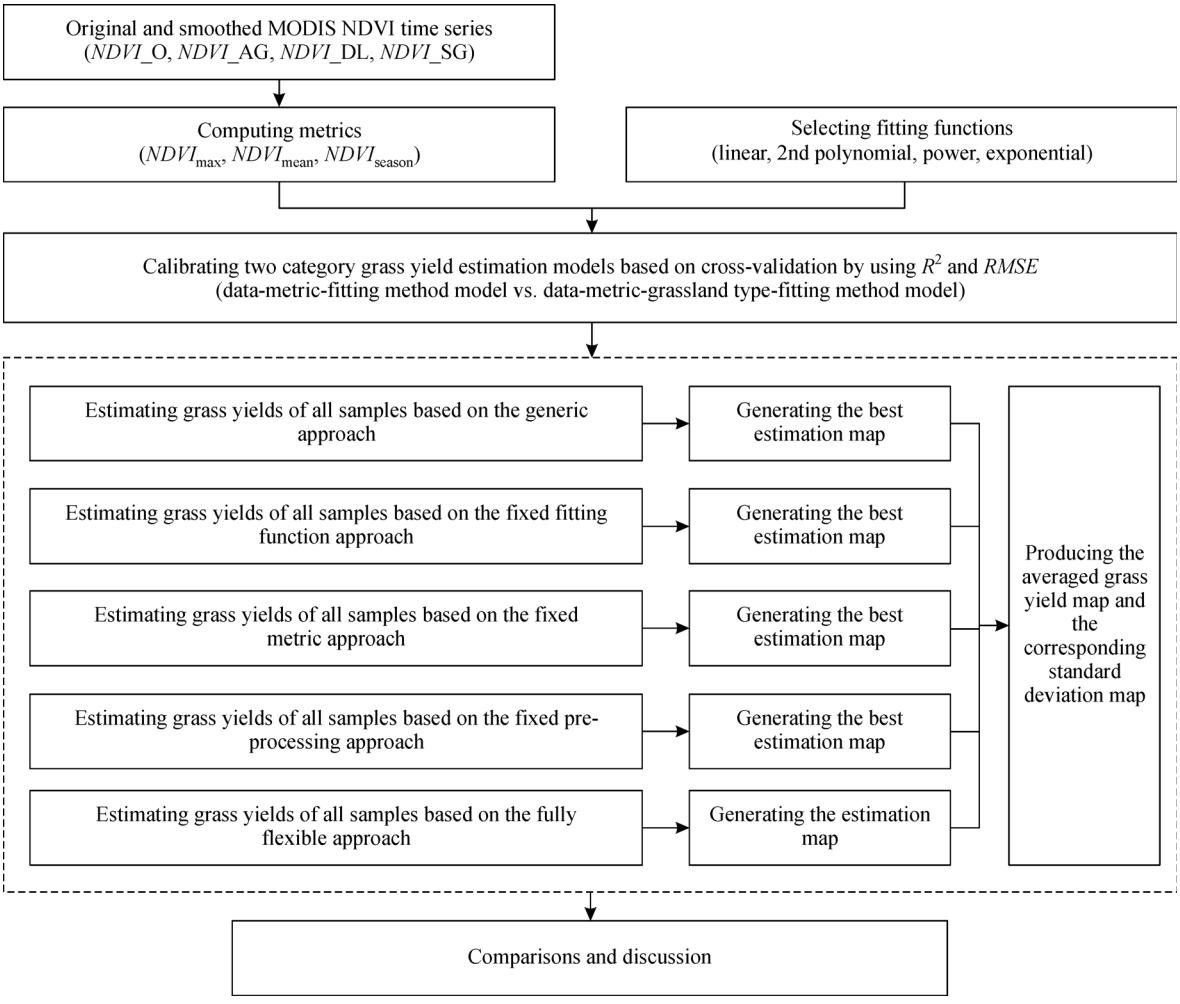

Fig. 3 Flowchart of the study.

Table 2 Summary of the five different approaches examined for grass yield estimation

Approaches	Grassland type-specific	Fixed parameters in each model	Flexible parameters in each model
Generic approach	No	Fitting coefficients Type of fitting function Metric Pre-processed data	None
Fixed fitting function approach	Yes	Type of fitting function Metric Pre-processed data	Fitting coefficients
Fixed metric approach	Yes	Metric Pre-processed data	Type of fitting function Fitting coefficients
Fixed pre-processing approach	Yes	Pre-processed data	Metric Type of fitting function Fitting coefficients
Fully flexible approach	Yes	None	Pre-processed data Metric Type of fitting function Fitting coefficients

estimation maps and analyzed their inconsistencies.

2.4.1 Accuracy assessment of models

To evaluate the performance of the two types of models, cross-validation was used, and two statistics were derived: R^2 and *RMSE*. The R^2 between measured and modeled grass yield is a common statistical measure which discriminates a 'good' from a 'bad' fit (Spiess and Neumeyer, 2010). After fitting, for the validation samples, the estimated yields and the ground observed yields should be linearly related. Therefore, R^2, *RMSE* and $RMSE_R$ were adopted as means to evaluate the accuracy, as Eqs. (1)–(3):

$$R^2 = \frac{\mathrm{cov}(Y,\hat{Y})^2}{\mathrm{var}(Y)\mathrm{var}(\hat{Y})}, \quad (1)$$

$$RMSE = \sqrt{\frac{\sum_{j=1}^{m}(Y_j - \hat{Y}_j)^2}{m}}, \quad (2)$$

$$RMSE_{\mathrm{R}} = \frac{RMSE}{\overline{Y}}, \quad (3)$$

where Y denotes the observed fresh grass yields of all validation samples, $\hat{Y}$ stands for the estimated fresh grass yields of all validation samples, m is the number of validation samples, Y_j is the observed fresh grass yield of the jth validation sample (kg/ha), $\hat{Y}_j$ is the estimated fresh grass yield of the jth validation sample (kg/ha) and $\overline{Y}$ is the mean of Y.

Since there were less than 30 samples for three classes, i.e., alpine meadow-steppe, temperate desert, and alpine meadow-high (Table 1), 5-fold cross-validation was done for these three types. For the remaining four grassland types, 10-fold cross-validation was used. For both types of models, the calibration was conducted based on the input pre-processing, metric and fitting function. We ran the cross-validation ten times, and recorded the mean values of R^2 and $RMSE_{\mathrm{R}}$. At the same time, we also recorded the optimum fitting coefficients for each specific model. The mean R^2 and $RMSE_{\mathrm{R}}$ were used for model selection in the next step and the coefficients were used when investigating the overall estimation accuracy and also for producing the estimation maps.

2.4.2 Summary of different empirical modeling approaches

After calibrating, we investigated the overall accuracy across all samples. To investigate the overall estimation accuracy, we designed five different approaches to produce the overall estimation in the order of increased flexibility in inputs (Table 2):

- **The generic approach**: estimated all available samples while ignoring grassland types, with all samples sharing the same coefficients. The generic approach essentially yields one model fitted across all grassland types, with one set of fitting coefficients.
- **The fixed fitting function approach**: estimated all available samples by estimating each grassland type separately with the same fitting function, as well as metric and pre-processing. Compared to the generic approach, however, each grassland type is modeled separately, with different fitting coefficients.
- **The fixed metric approach**: estimated all available samples with the same metrics for all grassland types, but using different fitting functions. The fitting function for a specific grassland type was selected according to the averaged R^2 and *RMSE* derived from cross validation. Sometimes, two or more fitting functions presented very close accuracy, then we chose one of them in the order of exponential > power > 2nd order polynomial > linear.
- **The fixed pre-processing approach**: estimated all available samples using the same pre-processing of data across grassland types, but using different metrics and fitting functions. The metric and fitting function for each specific grassland type was selected by examining the averaged R^2 and *RMSE* derived from cross validation. Sometimes, there were different combinations with very close accuracies, and we just randomly selected one combination.
- **The fully flexible approach**: estimated all available samples with fully variable inputs (pre-processings, metrics, fitting functions) for each grassland type in order to achieve the highest estimation accuracy. We examined the recorded cross-validation results, and selected the best combination to estimate grass yield of each grassland type.

After estimating the yield of all samples using the five approaches described above, we computed the overall estimation accuracy using R^2 and *RMSE*. The formulas were the same as Eqs. (1)–(2), except that all samples were adopted this time.

3 Results

3.1 Estimating grass yields of all samples

3.1.1 Generic approach

The generic approach estimated all available samples by ignoring the respective grassland type. Figure 4 shows the results of generic models for 12 different data inputs. Among the four fitting functions, the linear function presented the poorest results, with low R^2 and high *RMSE*. In contrast, the 2nd order polynomial model, power model, and exponential model achieved better results, with higher R^2 and lower *RMSE*. Among the four pre-processings, the original *NDVI* and the SG-smoothed *NDVI* performed best, in particular when combined with $NDVI_{\mathrm{season}}$. In most cases, $NDVI_{\mathrm{max}}$ yielded the poorest accuracies. Overall, among the three metrics, $NDVI_{\mathrm{season}}$ produced the best estimations no matter which pre-processing was used. In this scenario, the highest overall estimation accuracy was achieved by $NDVI\_O_{\mathrm{season}}$ and $NDVI\_SG_{\mathrm{season}}$ when using the exponential function, with R^2 of 0.52 and *RMSE* of 1214 kg/ha.

3.1.2 Fixed fitting function approach

The fixed fitting function approach was conducted for each grassland type separately. The results are presented in Fig. 5. Compared to the generic approach (Fig. 4), a

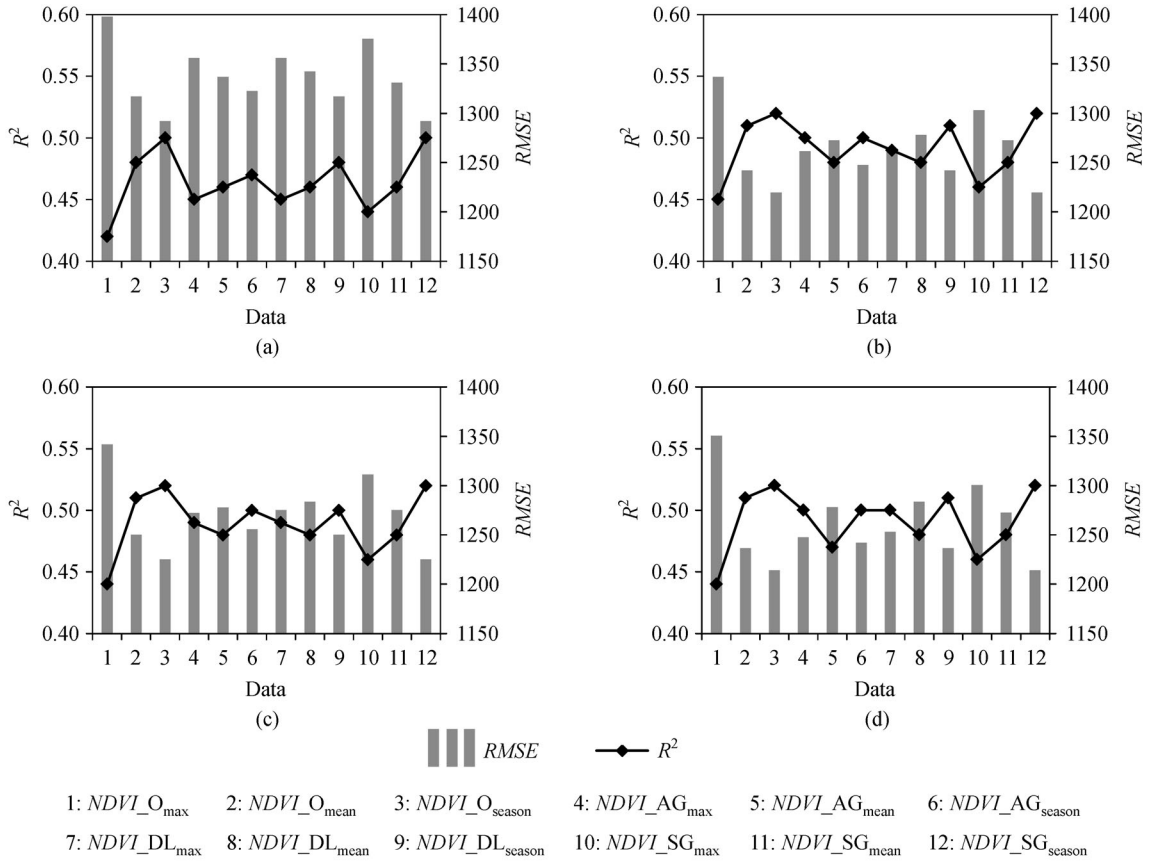

Fig. 4 Estimating grass yields based on the generic approach using (a) linear function, (b) 2nd polynomial function, (c) power function and (d) exponential function.

significant increase in accuracy was found across all fitting functions. 2nd order polynomial and the exponential functions performed well, in particular if combined with $NDVI_{season}$. The $NDVI_{max}$ also gave acceptable results, but only with AG- and DL-smoothed *NDVI* data. The highest accuracy was achieved by $NDVI\_O_{season}$ using exponential function, with R^2 approaching 0.54 and *RMSE* of 1174 kg/ha. Our findings confirm other studies (Xu et al., 2008; Schucknecht et al., 2017) which demonstrated that improved estimation accuracies can be obtained by differentiating grassland types or growth conditions.

3.1.3 Fixed metric approach

In the fixed metric approach each grassland type is modeled separately using different fitting functions but with fixed metrics. Results presented in Fig. 6 show that four combinations of metrics and pre-processings outperform the others (in decreasing order): $NDVI\_O_{season} > NDVI\_AG_{max} > NDVI\_O_{mean} > NDVI\_DL_{max}$. These four models reach R^2 of almost 0.55 with $RMSE \leqslant 1200$ kg/ha. The best estimation was achieved by $NDVI\_O_{season}$, with R^2 of 0.55 and *RMSE* of 1173 kg/ha. However, compared to the best estimation of the fixed fitting function approach (Section 3.1.2), the accuracy was not improved significantly.

3.1.4 Fixed pre-processing approach

In the fixed pre-processing approach, metrics and fitting functions can vary per grassland type but not the type of data pre-processing. The results are presented in Fig. 7 and show that this additional flexibility leads to a drastic decrease in *RMSE* across the four pre-processings. This decrease can be well seen when comparing Figs. 6 and 7. Best results were obtained using the original *NDVI*, followed by the DL-smoothed *NDVI*. However, models using SG- and AG- smoothed *NDVI* were only slightly worse compared to the two best performing pre-processings. The highest accuracy was achieved by $NDVI\_O$, with R^2 of 0.55 and *RMSE* of 1163 kg/ha.

3.1.5 Fully flexible approach

In the fully flexible approach, the data, metrics, and fitting functions used in fitting each grassland type were selected from the best performance of the cross-validation (inputs

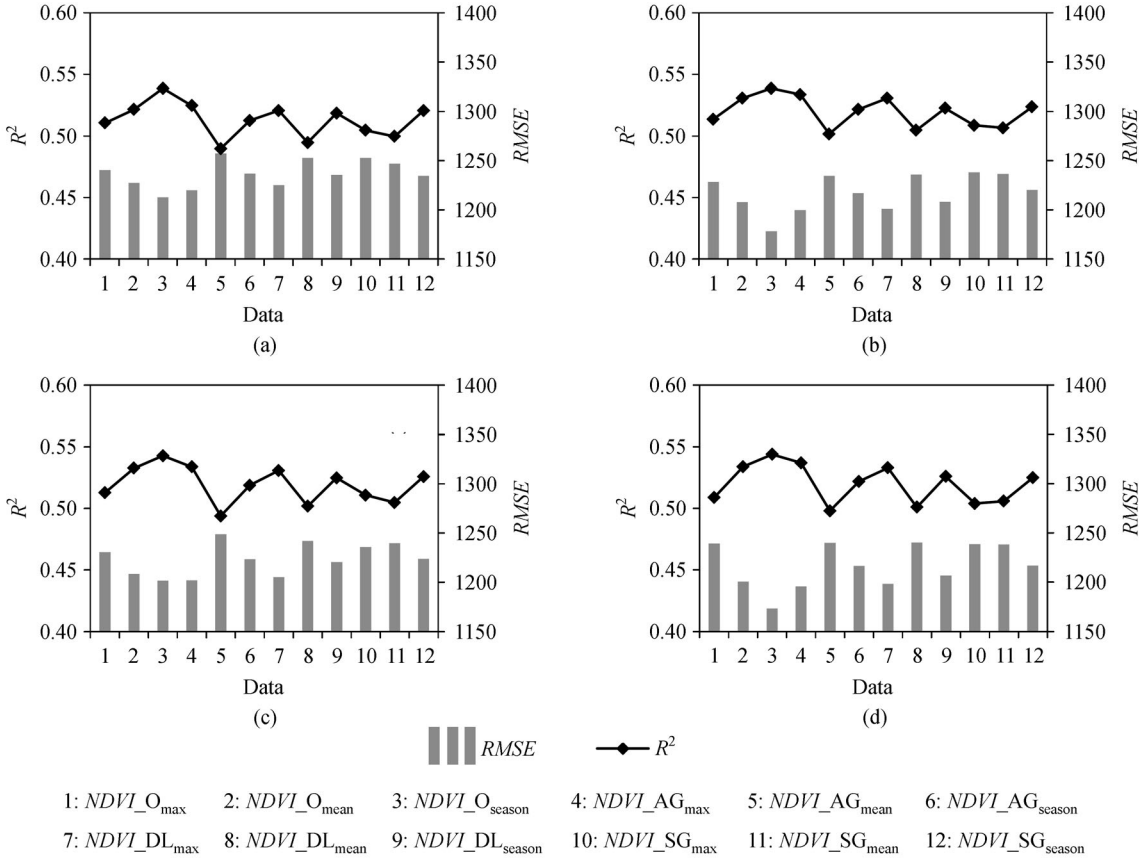

Fig. 5 Estimating grass yields based on the fixed function approach using (a) linear function, (b) 2nd order polynomial function, (c) power function and (d) exponential function.

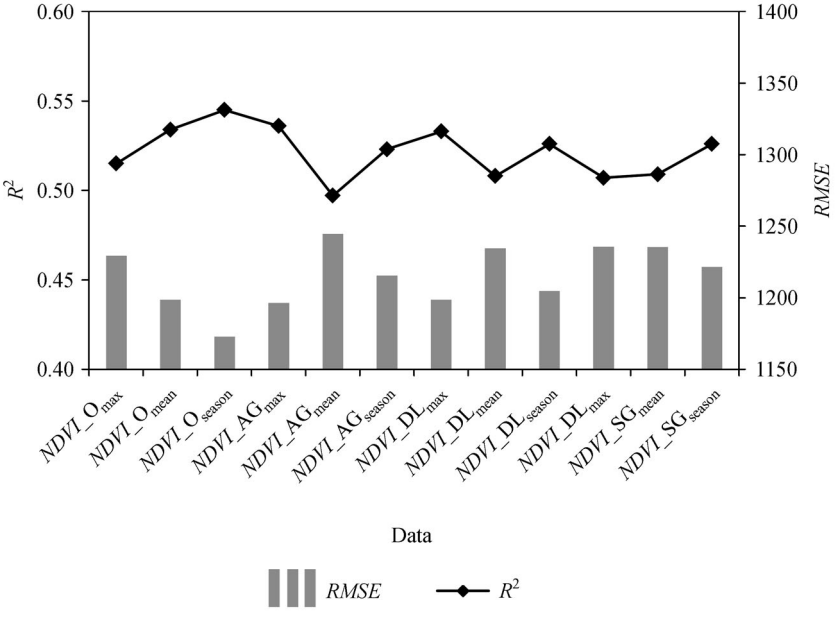

Fig. 6 Estimating grass yields based on the fixed metric approach.

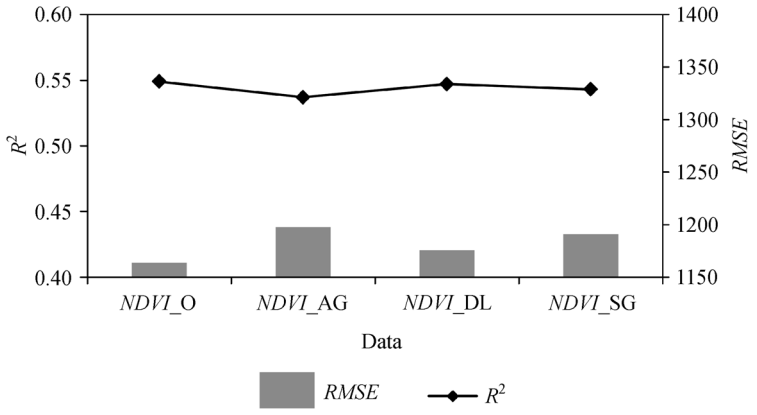

Fig. 7 Modeling grass yield based on the fixed pre-processing approach.

and fitting functions are shown in Table 3). With the fully flexible approach we obtained a R^2 of 0.57 and *RMSE* of 1140 kg/ha. Compared to the estimation using the generic model (3.1.1), this is a significant improvement. With respect to the other three more or less flexible approaches, the improvements are only minor (Table 3).

In addition to Table 3, Fig. 8 also provided scatterplots between the observed and the estimated grass yields of all samples using different approaches. Though generally similar, the relationships between the observed and estimated grass yields of the fully flexible approach are closer to 1:1 line than that of the generic approach,

Table 3 Formula and accuracy of the best estimation model in each approach

Approaches	Best estimation models	Formulas	R^2	*RMSE*/(kg·ha^{-1})
Generic approach	*NDVI*_O_{season} with exponential function	$Y = 314.862 \times e^{0.192 \times NDVI\_Oseason}$	0.52	1214
Fixed fitting function approach	*NDVI*_O_{season} with exponential function	1: $Y = 516.9 \times e^{0.142 \times NDVI\_Oseason}$ 2: $Y = 307.4 \times e^{0.156 \times NDVI\_Oseason}$ 3: $Y = 262.3 \times e^{0.221 \times NDVI\_Oseason}$ 4: $Y = 247.7 \times e^{0.250 \times NDVI\_Oseason}$ 5: $Y = 479.1 \times e^{0.165 \times NDVI\_Oseason}$ 6: $Y = 371.3 \times e^{0.164 \times NDVI\_Oseason}$ 7: $Y = 388.3 \times e^{0.170 \times NDVI\_Oseason}$	0.54	1174
Fixed metric approach	*NDVI*_O_{season} with different functions	1: $Y = 516.9 \times e^{0.142 * NDVI\_Oseason}$ 2: $Y = -374.2 + 187.6 \times NDVI\_O_{season}$ 3: $Y = 89.6 \times (NDVI\_O_{season})^{1.419}$ 4: $Y = 247.7 \times e^{0.250 \times NDVI\_Oseason}$ 5: $Y = 479.1 \times e^{0.165 \times NDVI\_Oseason}$ 6: $Y = 371.3 \times e^{0.164 \times NDVI\_Oseason}$ 7: $Y = 388.3 \times e^{0.170 \times NDVI\_Oseason}$	0.55	1173
Fixed pre-processing approach	*NDVI*_O with different metrics and fitting functions	1: $Y = 4264.0 \times (NDVI\_s)^{1.484}$ 2: $Y = 8114.0 \times (NDVI\_O_{mean})^{1.384}$ 3: $Y = 67.2 \times (NDVI\_O_{season})^{1.348}$ 4: $Y = 247.7 \times e^{0.250 \times NDVI\_Oseason}$ 5: $Y = 479.1 \times e^{0.165 \times NDVI\_Oseason}$ 6: $Y = 13353.0 \times (NDVI\_O_{mean})^{1.645}$ 7: $Y = 2957.1 - 10326.0 \times NDVI\_O_{max} + 13526.0 \times (NDVI\_O_{max})^2$	0.55	1163
Fully flexible approach		1: $Y = 366.0 \times e^{2.856 \times NDVI\_DLmax}$ 2: $Y = 95.3 \times (NDVI\_SG_{season})^{1.170}$ 3: $Y = 4356.9 \times (NDVI\_AG_{max})^{1.419}$ 4: $Y = 247.7 \times e^{0.250 \times NDVI\_Oseason}$ 5: $Y = 479.0 \times e^{0.165 \times NDVI\_Oseason}$ 6: $Y = 192.4 \times e^{3.228 \times NDVI\_SGmax}$ 7: $Y = 4819.9 - 44035.6 \times NDVI\_DL_{mean} + 115798.5 \times (NDVI\_DL_{mean})^2$	0.57	1140

Note: Grassland types: 1: temperate steppe; 2: alpine meadow-steppe; 3: alpine steppe; 4: temperate desert; 5: alpine meadow-low; 6: alpine meadow-medium; 7: alpine meadow-high.

especially for temperate steppe and alpine meadow-low, the improvement is obvious. However, the relationship of alpine meadow-medium is not greatly improved, probably it needs further division of the group, or maybe grass yields cannot be well explained by *NDVI* only in this region. Multivariate approaches are something to consider in future studies, combining more factors such as temperature, precipitation, aspect, and solar radiation.

3.2 Modeling grass yields over the whole area

Though we already investigated the overall accuracies of different approaches using cross-validated statistics, we also checked the resulting spatial patterns of grass yields over the entire Qinghai Province. To do so, we modeled the grass yields with the best estimation models listed in Table 3. Figure 9(a) shows the mean grass yields from the five approaches and its standard deviations. The modeled yields are closely related to the spatial distribution of the seven grassland types (see Fig. 1 for comparison), but shows more spatial details. High production areas (>3000 kg/ha) were mainly distributed in the alpine meadow-low in the east. Medium production areas (1200–3000 kg/ha) were predominantly found in the temperate steppe and alpine meadow-medium in the south and east. Low production areas (<1200 kg/ha) were mainly distributed in the alpine meadow-high, alpine meadow-steppe, alpine steppe, and temperate desert in the center and west. Standard deviation map (Fig. 9(b)) shows grass yields derived from the five approaches agreed with each other well. The standard deviation of most grasslands is less than 200 kg/ha. Combined with Fig. 1, it is quite clear that grassland with high standard deviation (>500 kg/ha) are concentrated in alpine meadow-medium and alpine meadow-high.

Existing regional discrepancies in grass yields between the five approaches are further detailed in Fig. 10 for the small area denoted with the red box in Fig. 9. In Fig. 10(a) to Fig. 10(c), results were relatively consistent with each other. In Figs. 10(d)–10(e), however, we allowed different metrics and even different pre-processings to be used in the estimations of each grassland type. This additional flexibility reduced on one hand the cross-validated error statistics (Figs. 6 and 7) but resulted in highly unrealistic yield estimates in the areas classified as alpine meadow-high (Fig. 11). Considering the natural conditions and by examining the *NDVI* time series, it is highly doubtful that this area could output such high yields. Thus, we further calculated the histograms of alpine meadow-high and alpine steppe in Fig. 10(d), the results are shown in Fig. 12 (a). These two classes within the red box show almost the same data distribution. Either the grassland type had been

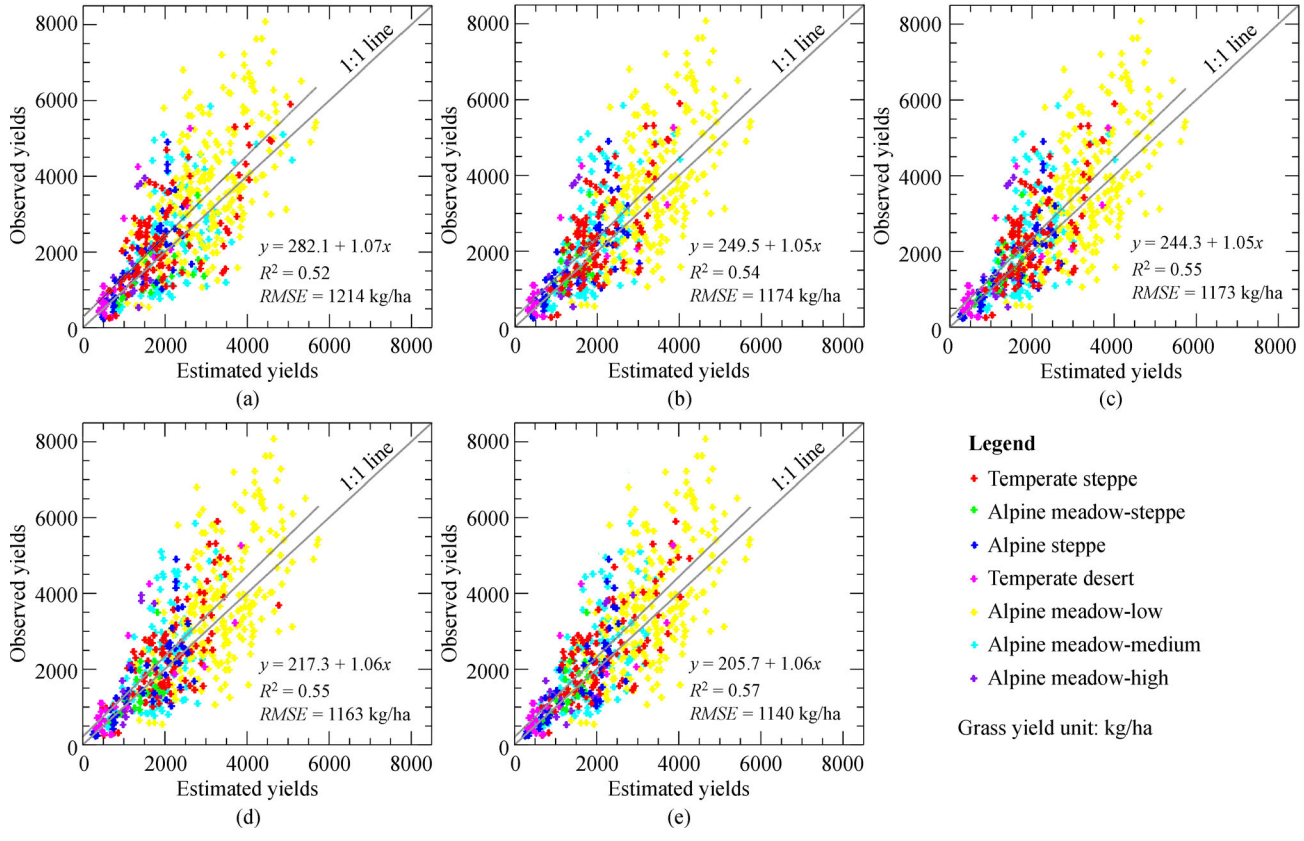

Fig. 8 Scatter plots of the best estimation models of the five approaches as listed in Table 3. (a) generic approach, (b) fixed fitting function approach, (c) fixed metric approach, (d) fixed pre-processing approach, (e) fixed pre-processing approach.

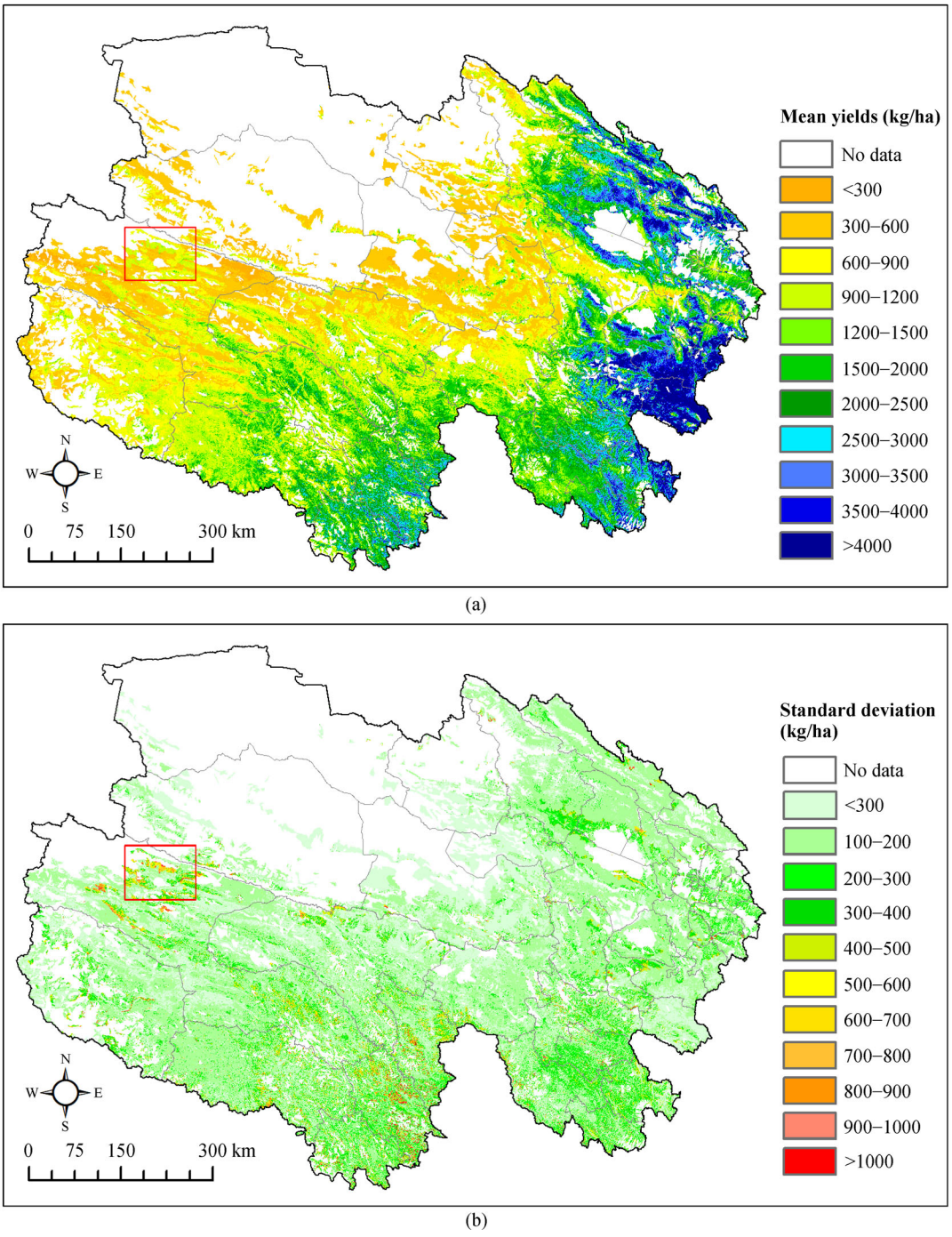

Fig. 9 (a) Mean and (b) standard deviation of the modeled grass yields for research area using the five approaches listed in Table 3. Red box indicates region of high standard deviations.

misclassified in this area, or the yield model was not appropriate for producing a yield map. Further, we draw samples and the fitted formula used to model alpine meadow-high and alpine steppe in Fig. 10(d). It can be seen in Fig. 12(b), *NDVI* value of the samples within alpine meadow-high ranges from 0.35 to 0.8. However, if this formula is used to estimate pixels with values < 0.3, it will produce unexpected high production. In this area, the yield model had to extrapolate far beyond the *NDVI* values seen in the calibration data set.

4 Discussion

Overall, the *RMSE*s of all models listed in Table 3 are lower than the standard deviation of all samples as shown

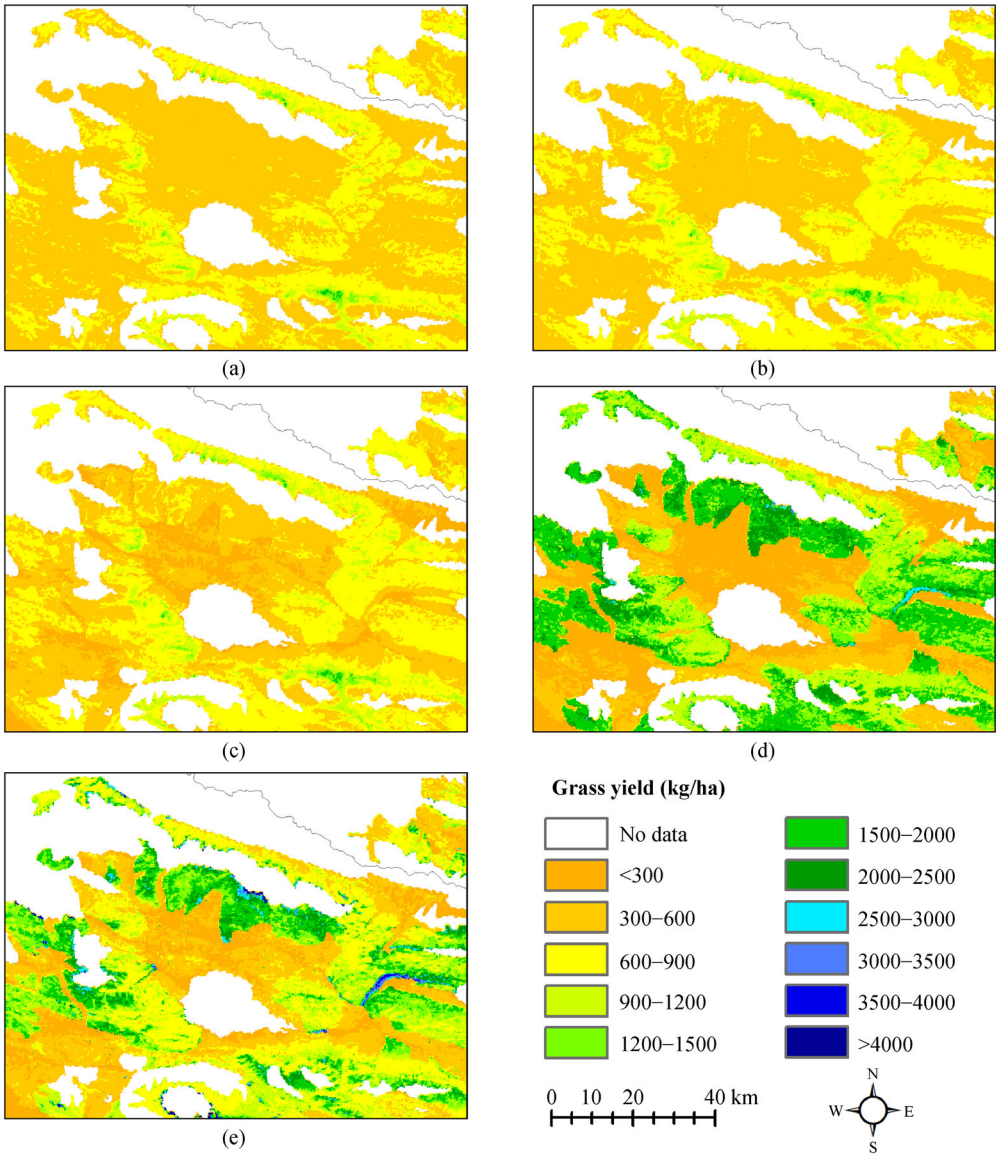

Fig. 10 Zoom-in comparison of the modeled grass yields in the red box as shown in Fig. 9. (a)–(e) are grass yield maps derived from the best estimation of each approach listed in Table 3. (a) The generic approach, (b) the fixed fitting function approach, (c) the fixed metric approach, (d) the fixed pre-processing approach, and (e) the fully flexible approach.

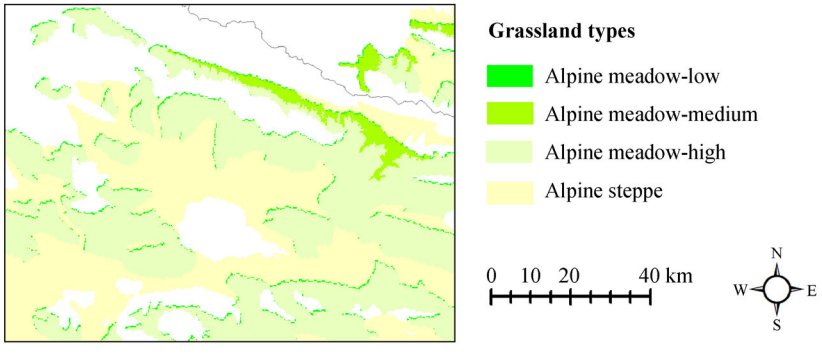

Fig. 11 Grassland types within the red box shown in Fig. 9. The extent corresponds to Fig. 10.

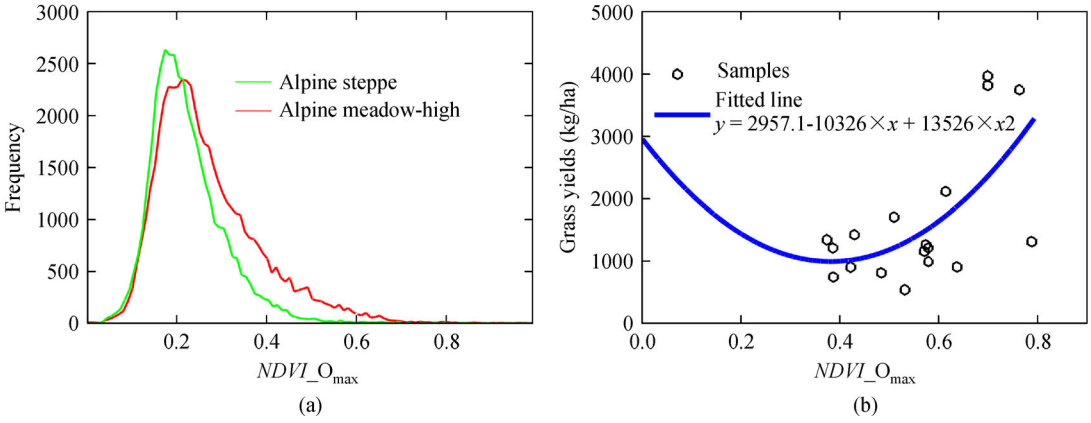

Fig. 12 (a) histograms of the pixels within alpine meadow-high and alpine steppe shown in Fig. 10(d), and (b) samples and the fitted line of alpine meadow-high.

in Table 1 (1644.63 kg/ha). The estimation accuracies in this study are also comparable to existing studies covering Qinghai province. For example, Xu et al. (2008) modeled the dry grass yields with *NDVI* in the six major grassland regions of China during 2004 and 2005, their model *RMSE* for areas covering Qinghai was 594 kg/ha. As the conversion coefficient from dry grass yield to fresh grass yield ranges from 2.5 to 3.5 in this area (Department of Agriculture, Animal Husbandry and Animal Husbandry and Veterinary of the People's Republic of China and General Animal Husbandry and Veterinary Station of China, 1996), the corresponding *RMSE* of fresh yield ranges from 1485 kg/ha to 2079 kg/ha. Therefore, the *RMSE* of our study is lower than their findings. Zhang et al. (2017) estimated the aboveground biomass of Qilian County, a county located in the north-east of Qinghai Province, in 2014. Their modeled *RMSE* was 1713.4 kg/ha. Considering most of the grassland in Qilian County is a high production type (alpine meadow-low), this *RMSE* is acceptable. Since we modeled both low and high production types in our study, it is quite reasonable that the *RMSE* of our model is lower. Feng et al. (2011) modeled grass yields of five provinces in the north-west and south-west of China including Qinghai during 2005–2006. They used the generic approach and the best accuracy was obtained with *NDVI* and the exponential model, with R^2 of 0.51 and *RMSE* of 2595.21 kg/ha. Considering most of their ground samples were located in Qinghai Province, their results can be served as a contrast, and our *RMSE* is much lower than theirs.

In our study, we found that grass yields estimation accuracy increased step by step with the increased flexibility in different approaches. Compared with the generic approach, there was an obvious increase in R^2 and an obvious decrease in *RMSE* of the estimation accuracy, by means of modeling each grassland type separately (the fixed fitting function approach). In contrast, there was only a small increase in R^2 of the estimation accuracy, in terms of using different fitting functions (the fixed metric approach). And there was only a small decrease in *RMSE* of the estimation accuracy by using different metrics (the fixed processing approach). Finally, the estimation accuracy improved greatly if given full flexibility in choosing input variables (the fully flexible approach). Though the fully flexible approach presented the best estimation accuracy, there are two issues with this method. One is that there are too many variables that need to be computed or processed in this approach which will inevitably increase the workload. The balance between accuracy and workload should be considered. The second is the over-fit problem. Though accuracy based on samples may be very high, but when the model is applied to regions, the results may contain unexpected errors. A better way is to check the sample set and the data set before designing estimation models.

Though we considered different approaches to improve grass yields estimation accuracy, it is still region-specific and is not directly transferable to other regions. Ketzer et al. (2017) developed a GIS-based model to assess grassland biomass potentials for energy. Their model linked geospatial data (soil data, land cover, digital elevation model) with agricultural statistical data (grassland areas, animal number) (Haase et al., 2016). It provided improved quality and consistency in biomass assessment at different scales and different regions in the European Union. Since many geospatial data and agricultural statistical data are readily available or can be obtained from local authorities, their model can easily be improved and adopted to other regions. However, the potentials of the model in estimating grass yields remains to be explored in other regions.

5 Conclusions

The accurate estimation of grass yield over large areas is of

great importance in grassland-related research. To evaluate the impact of several methodological choices, we considered four commonly used pre-processing techniques, four fitting functions, and three *NDVI* metrics (VI_{max}, VI_{mean}, VI_{season}). The assessment was based on two model assessment criteria (R^2 and *RMSE*) calculated over 556 reference samples in a 5 to 10-fold cross validation. In our assessments, we also considered and evaluated the impact of using pre-existing grassland type maps for stratified modeling. In general, we found that MODIS coarse resolution *NDVI* time series were suitable for large scale mapping of grassland biomass. The Qinghai grasslands cover almost 42 million ha, and despite this size, we were able to achieve satisfactory accuracies (R^2 = 0.57 and *RMSE* = 1140 kg/ha) against 556 reference samples spread over the province. Results also show that our proposed approaches yielded acceptable accuracies when compared with existing studies.

The impacts of all the variables considered in this study to the final modeled grass yield map were discussed. As a conclusion, better study of the sample range and the image range are needed before the estimation and one should be cautious when selecting fitting functions. Though data filtering did not present an increase in accuracy in this study, it may still need to produce grass yield maps with good continuity. In the end, we recommend to use either the "fixed fitting function" approach or "fixed metric" approach. The two approaches permit some flexibility with respect to the respective grassland type, but use the same *NDVI* metric.

Acknowledgements This research was supported by the National Natural Science Foundation of China (Grant No. 41401494), National Key Research and Development Plan (No. 2017YFC0404302), and Talented Youth Project of Hebei Education Department (No. BJ2018043).

References

Ali I, Cawkwell F, Dwyer E, Barrett B, Green S (2016). Satellite remote sensing of grasslands: from observation to management. J Plant Ecol, 9(6): 649–671

Atkinson P M, Jeganathan C, Dash J, Atzberger C (2012). Inter-comparison of four models for smoothing satellite sensor time-series data to estimate vegetation phenology. Remote Sens Environ, 123: 400–417

Atzberger C, Darvishzadeh R, Immitzer M, Schlerf M, Skidmore A, le Maire G (2015). Comparative analysis of different retrieval methods for mapping grassland leaf area index using airborne imaging spectroscopy. Int J Appl Earth Obs, 43: 19–31

Baret F, Buis S (2008). Estimating canopy characteristics from remote sensing observations: review of methods and associated problems., Advances in Land Remote Sensing: Springer, 173–201

Baret F, Guyot G (1991). Potentials and limits of vegetation indices for LAI and APAR assessment. Remote Sens Environ, 35(2–3): 161–173

Baret F, Guyot G, Major D J (1989). Crop biomass evaluation using radiometric measurements. Photogrammetria, 43(5): 241–256

Beck P S A, Atzberger C, Høgda K A, Johansen B, Skidmore A K (2006). Improved monitoring of vegetation dynamics at very high latitudes: a new method using MODIS NDVI. Remote Sens Environ, 100(3): 321–334

Chen H, Zhu Q, Peng C, Wu N, Wang Y, Fang X, Gao Y, Zhu D, Yang G, Tian J, Kang X, Piao S, Ouyang H, Xiang W, Luo Z, Jiang H, Song X, Zhang Y, Yu G, Zhao X, Gong P, Yao T, Wu J (2013). The impacts of climate change and human activities on biogeochemical cycles on the Qinghai-Tibetan Plateau. Glob Change Biol, 19(10): 2940–2955

Chen J, Jönsson P, Tamura M, Gu Z, Matsushita B, Eklundh L (2004). A simple method for reconstructing a high-quality *NDVI* time-series data set based on the Savitzky-Golay filter. Remote Sens Environ, 91 (3–4): 332–344

Darvishzadeh R, Atzberger C, Skidmore A, Schlerf M (2011). Mapping grassland leaf area index with airborne hyperspectral imagery: a comparison study of statistical approaches and inversion of radiative transfer models. Isprs J Phtogramm, 66(6): 894–906

Darvishzadeh R, Skidmore A, Schlerf M, Atzberger C (2008). Inversion of a radiative transfer model for estimating vegetation LAI and chlorophyll in a heterogeneous grassland. Remote Sens Environ, 112 (5): 2592–2604

de Smith M J, Goodchild M F, Longley P A (2018). Geospatial Analysis: A Comprehensive Guide (Sixth edition): Winchelsea Press Department of Agriculture, Animal Husbandry and Veterinary of the People's Republic of China, General Animal Husbandry and Veterinary Station of China (1996). China Grassland Resources. Beijing: China Science and Technology Press

Duan M, Gao Q, Wan Y, Li Y, Guo Y, Ganzhu Z, Liu Y, Qin X (2012). Biomass estimation of alpine grasslands under different grazing intensities using spectral vegetation indices. Can J Remote Sens, 37 (4): 413–421

Feng Q, Gao X, Huang X, Yu H, Liang T (2011). Remote sensing dynamic monitoring of grass growth in Qinghai-Tibet Plateau from 2001 to 2010. J Lanzhou U, 47(4): 75–81

Fu X, Tang C, Zhang X, Zhang X, Zhou S, Huang Y, Jiang D (2013). Estimation of grass yield based on MODIS data in Sichuan Province, China. J Earth Inform Sci, 15(4): 611–617

Gao F, Morisette J T, Wolfe R E, Ederer G, Pedelty J, Masuoka E, Myneni R, Tan B, Nightingale J (2008). An algorithm to produce temporally and spatially continuous MODIS-LAI time series. IEEE Geosci Remote S, 5(1): 60–64

Haase M, Rösch C, Ketzer D (2016). GIS-based assessment of sustainable crop residue potentials in European regions. Biomass Bioenerg, 86: 156–171

Hird J N, McDermid G J (2009). Noise reduction of *NDVI* time series: an empirical comparison of selected techniques. Remote Sens Environ, 113(1): 248–258

Huete A, Didan K, Miura T, Rodriguez E P, Gao X, Ferreira L G (2002). Overview of the radiometric and biophysical performance of the MODIS vegetation indices. Remote Sens Environ, 83(1–2): 195–213

Jenks G F, Caspall F C (1971). Error on choroplethic maps: definition, measurement, reduction. Ann Assoc Am Geogr, 61(2): 217–244

Jönsson P, Eklundh L (2002). Seasonality extraction by function-fitting to time series of satellite sensor data. IEEE T Geosci Remote, 40(8):

1824–1832
Jordan C F (1969). Derivation of leaf-area index from quality of light on the forest floor. Ecology, 50(4): 663–666
Ketzer D, Rösch C, Haase M (2017). Assessment of sustainable Grassland biomass potentials for energy supply in Northwest Europe. Biomass Bioenerg, 100: 39–51
Klisch A, Atzberger C (2016). Operational drought monitoring in Kenya using MODIS *NDVI* time series. Remote Sens (Basel), 8(4): 267
Li J, Liang T, Chen Q (1998). Estimating grassland yields using remote sensing and GIS technologies in China. New Zeal J Agr Res, 41(1): 31–38
Li X, Li M, Dong S, Shi J (2015). Temporal-spatial changes in ecosystem services and implications for the conservation of alpine rangelands on the Qinghai-Tibetan Plateau. Rangeland J, 37(1): 31–43
Lobell D B, Asner G P (2004). Cropland distributions from temporal unmixing of MODIS data. Remote Sens Environ, 93(3): 412–422
Mohammat A, Wang X, Xu X, Peng L, Yang Y, Zhang X, Myneni R B, Piao S (2013). Drought and spring cooling induced recent decrease in vegetation growth in Inner Asia. Agr Forest Meteorol, 178–179: 21–30
Pearson R L, Miller L D (1972). Remote mapping of standing crop biomass for estimation of the productivity of the shortgrass prairie. Remote Sens Environ, VIII: 7–12
Piao S, Fang J, Zhou L, Tan K, Tao S (2007). Changes in biomass carbon stocks in China's grasslands between 1982 and 1999. Global Biogeochem Cy, 21(2)
Piao S, Mohammat A, Fang J, Cai Q, Feng J (2006). *NDVI*-based increase in growth of temperate grasslands and its responses to climate changes in China. Glob Environ Change, 16(4): 340–348
Pinzon J E, Tucker C J (2010). GIMMS 3g *NDVI* set and global *NDVI* trends. In: Second Yamal Land-Cover Land-Use Change Workshop. Finland: Rovaniemi, 8–10
Qi J, Chehbouni A, Huete A R, Kerr Y H, Sorooshian S (1994). A modified soil adjusted vegetation index. Remote Sens Envrion, 48 (2): 119–126
Qinghai Provincial Grassland Station (2012). Qinghai Grassland Resources. Xining: Qinghai People's Publishing House
Rembold F, Atzberger C, Savin I, Rojas O (2013). Using low resolution satellite imagery for yield prediction and yield anomaly detection. Remote Sens (Basel), 5(4): 1704–1733
Ren J, Chen Z, Zhou Q, Tang H (2008). Regional yield estimation for winter wheat with MODIS-*NDVI* data in Shandong, China. Int J Appl Earth Obs, 10(4): 403–413
Rojas O (2007). Operational maize yield model development and validation based on remote sensing and agro-meteorological data in Kenya. Int J Remote Sens, 28(17): 3775–3793
Rondeaux G, Steven M, Baret F (1996). Optimization of soil-adjusted vegetation indices. Remote Sens Environ, 55(2): 95–107
Roujean J L, Breon F M (1995). Estimating PAR absorbed by vegetation from bidirectional reflectance measurements. Remote Sens Environ, 51(3): 375–384
Rusch G M, Zapata P C, Casanoves F, Casals P, Ibrahim M, DeClerck F (2014). Determinants of grassland primary production in seasonally-dry silvopastoral systems in Central America. Agroforest Syst, 88(3): 517–526
Schucknecht A, Meroni M, Kayitakire F, Boureima A (2017). Phenology-based biomass estimation to support rangeland management in semi-arid environments. Remote Sens (Basel), 9(5): 463
Spiess A N, Neumeyer N (2010). An evaluation of R^2 as an inadequate measure for nonlinear models in pharmacological and biochemical research: a Monte Carlo approach. BMC Pharmacol, 10(1): 6
Tukey J W (1977). Exploratory Data Analysis. New York: Pearson
Vermote E F, Roger J C, Ray J P (2015). MODIS Surface Reflectance User's Guide-Collection 6
Wehlage C D, Gamon A J, Thayer D, Hildebrand V D (2016). Interannual variability in dry mixed-grass prairie yield: a comparison of MODIS, SPOT, and field measurements. Remote Sens (Basel), 8 (10): 872
Xu B, Yang X C, Tao W G, Qin Z H, Liu H Q, Miao J M, Bi Y Y (2008). MODIS-based remote sensing monitoring of grass production in China. Int J Remote Sens, 29(17–18): 5313–5327
Xue J, Su B (2017). Significant Remote sensing vegetation indices: a review of developments and applications. J Sensors, 2017(1353691): 1–17
Xun Q, Dong Y, An S, Yan K (2018). Monitoring of grassland herbage accumulation by remote sensing using MOD09 GA data in Xinjiang. Acta Pratacult Sin, 27(4): 10–26
Yang S, Zhang W, Feng Q, Meng B, Gao J, Liang T (2016). Monitoring of grassland herbage accumulation by remote sensing using MODIS daily surface reflectance data in the Qingnan Region. Acta Pratacult Sin, 25(8): 14–26
Yin F, Deng X, Jin Q, Yuan Y, Zhao C (2014). The impacts of climate change and human activities on grassland productivity in Qinghai Province, China. Front Earth Sci-PRC, 8(1): 93–103
Yu L, Zhou L, Liu W, Zhou H (2010). Using remote sensing and GIS technologies to estimate grass yield and livestock carrying capacity of alpine grasslands in Golog prefecture, China. Pedosphere, 20(3): 342–351
Zhang F, Wang H, Zhu Y, Zhang Z, Li X (2017). Study on the aboveground biomass of natural grassland and balance between forage and livestock in Qilian County. J Nat Resour, 7(32): 1183–1192
Zhou L M, Tucker C J, Kaufmann R K, Slayback D, Shabanov N V, Myneni R B (2001). Variations in northern vegetation activity inferred from satellite data of vegetation index during 1981 to 1999. J Geophys Res-Atmos, 106(D17), 20069–20083

AUTHORS BIOGRAPHIES

Jianhong Liu is an associate professor at Northwest University. She received her BS degree in geographic information system from Wuhan University in 2008, and her PhD degree in cartography and geographic information system from Beijing Normal University in 2013. Her current research interests include remote sensing image analysis and its applications in agricultural monitoring and land cover/land use change detection.

Clement Atzberger is a professor at the University of Natural Resources and Life Science, Vienna. He is head of the Institute of

Surveying, Remote Sensing and Land Information. He is an expert at remote sensing image processing, radiative transfer modeling, vegetation monitoring, time series analysis, land use and land cover classification.

Xin Huang is an undergraduate student at the Northwest University and his major is geography. His research interest is remote sensing applications in land use/land cover change monitoring.

Kejian Shen is a senior engineer at Chinese Academy of Agricultural Engineering Planning and Design. He received his BS degree in land resource management from Hebei Agricultural University in 2005, his Master degree in physical geography from China University of Geosciences (Beijing), and his PhD degree in cartography and geographic information system from Beijing Normal University in 2012. His current research interests include remote sensing image analysis and its applications in agricultural monitoring, and land cover/land use change detection.

Yongmei Liu is an associate professor at Northwest University. She received her BS degree in physical geography from Northwest University in 1992, and her PhD degree in soil science from Institute of Soil and Water Conservation, China Academy of Science in 2006. Her current research interests include hyperspectral remote sensing of vegetation, vegetation index analysis and vegetation change detection.

Lei Wang is an associate professor at Northwest University. He received his BS degree from Wuhan University in 1999, his MS degree from Northwest University in 2005, and his PhD degree from China Academy of Science in 2013. He is specialized in cartography, digital elevation modeling and GIS spatial analysis.